Surface plasmon resonance study of vesicle rupture by virus-mimetic attack

Soonwoo Chah† and Richard N. Zare*

Received 15th February 2008, Accepted 4th April 2008
First published as an Advance Article on the web 21st April 2008
DOI: 10.1039/b802632g

Frank and coworkers [N. J. Cho, S. J. Cho, K. H. Cheong, J. S. Glenn and C. W. Frank, *J. Am. Chem. Soc.*, 2007, **129**, 10050] investigated what happens when lipid vesicles made of POPC (1-palmitoyl-2-oleoyl-*sn*-glycero-3-phosphocholine), which serves as a mimic for cell membranes, are exposed to the amphipathic helix peptide, PEP1, which is of the same type found in hepatitis C virus. Using atomic force field microscopy and quartz crystal microbalance measurements they presented evidence that the vesicle is transformed into a lipid bilayer. We use surface plasmon resonance (SPR) microscopy to follow this process in real time. We find an induction period (intermediate state) of ~10-min duration between the time of membrane binding and membrane rupture. The SPR data support the interpretation that a lipid bilayer is formed and allow us to put forward a mechanism for the vesicle-rupture event. As a side benefit, we demonstrate how to build two-dimensional lipid patterns on a gold surface using this vesicle-rupture process.

Introduction

We have presently a fair but incomplete understanding of the course of viral infection. When a virus invades a cell in the body, it begins by fusing with the cell's protective outer membrane, penetrating it, and ultimately releasing its genetic cargo inside the cell. This release turns the host cell into a chemical factory to produce more copies of the virus, which are disgorged later to attack other cells. The infection of a cell is unavoidable and often irreversible once a virus penetrates the cell membrane. Thus, scientists have tried to develop antiviral drugs that prevent or hinder the encounter. For this purpose, it is important to understand how the virus interacts with and breaks up the cell membrane. Knowledge of the exact sequence and duration of these steps is crucial to developing possible antiviral strategies for combating disease.

In recent years much progress has been made in following the virus–cell fusion event, which appears to have been accomplished exclusively by time-resolved fluorescence microscopy. Melikyan and co-workers[1,2] filmed individual viruses fusing with a host cell membrane using fluorescence microscopy. They detected an intermediate stage between the time a virus merges with the cell membrane and the time the microbe delivers its genetic contents into the cell. During this period the fate of the host cell hangs in the balance. Consequently, Melikyan and co-workers suggested that this intermediate stage, which can last several minutes, may represent a window of opportunity for drug development.

Department of Chemistry, Stanford University, Stanford, CA 94305-5080, USA. E-mail: zare@stanford.edu
† Present address: Intel Corporation, 2200 Mission College Blvd, Santa Clara, CA 95054, USA.

We investigated the intermediate stage more closely using surface plasmon resonance (SPR) microscopy. To better understand this stage, we simplified the system by using the interaction of an amphipathic helix peptide (AHP) with a lipid vesicle. Elazar *et al.*[3] identified an N-terminal amphipathic helix in NS5A, a nonstructural protein of hepatitis C virus (HCV). HCV is a positive, single-stranded RNA virus that causes significant morbidity and mortality, infecting over 100 million people worldwide. Elazar *et al.* found that the amphipathic helix in NS5A is necessary and sufficient for membrane localization. Cho *et al.*[4] recently reported a method to destabilize a collection of intact vesicles and to transform them into a planar bilayer structure using an AHP. These two papers suggested to us that PEP1, which is an AHP, and a 1-palmitoyl-2-oleoyl-*sn*-glycero-3-phosphocholine (POPC) vesicle would be a good model system to mimic virus attack of a cell. The investigation of the interaction of PEP1 AHP with the POPC vesicle has another meaning for the study of HCV because this interaction is known to impair the replication of this virus.

We chose the SPR technique for investigating the interaction because it is known to be quite sensitive in detecting lateral changes at the interface and does not require tagging materials that may possibly disturb or affect the interaction. After the injection of AHP onto vesicle layers, peptides were initially embedded in the vesicle surface in a parallel direction. Subsequently, it rearranged to form transmembrane peptide pores, which led to vesicle rupture. This attack caused the vesicle's transformation into a lipid bilayer. The SPR analysis, which provided optical properties of lipids in different formats (vesicles *versus* bilayers) helped us to understand how an AHP causes vesicle rupture and put forward a mechanism for this rupture event. As an added benefit, we demonstrate how to build two-dimensional lipid patterns on a gold surface using this vesicle-rupture mechanism.

Materials and methods

Preparation of 30-nm POPC vesicles

POPC was purchased from Avanti Polar Lipids (Alabaster, AL). It was initially dissolved in chloroform in a 10-ml vial, and then dried under nitrogen gas until all the solvents were removed. Next, it was stored in a desiccator under vacuum. Prior to use, the lipids in the vial were dissolved in Tris buffer, which is a mixture of 10 mM Tris, 150 mM NaCl, and 1 mM ethylene diaminetetraacetic acid (EDTA) in 18.2 MΩ cm MilliQ water (MilliPore). The lipids and Tris buffer were agitated with a vortex for 5 min, which resulted in the formation of multilamellar POPC vesicles. These vesicles were broken down to smaller unilamellar vesicles when passed through an extruder (Avanti Polar Lipids) equipped with a polycarbonate membrane filter having 30-nm-diameter holes. The concentration of vesicles was generally $\sim$5 mg mL^{-1} and it was diluted 10 times when used for experiments.

Amphipathic helix peptide PEP1

PEP1 was purchased from Anaspec Corporation (San Jose, CA). PEP1 is a synthetic peptide that mimics wild-type amphipathic helix and is known to inhibit membrane association of NS5A (nonstructural protein 5A of HCV), hence impairing HCV replication[3]. Its sequence is Ser–Gly–Ser–Trp–Leu–Arg–Asp–Val–Trp–Asp–Trp–Ile–Cys–Thr–Val– Leu–Thr–Asp–Phe–Lys–Thr–Trp–Leu–Gln–Ser–Lys–Leu–Asp–Tyr– Lys–Asp–NH_2 (MW 3805.3).

Preparation of plasma-treated gold substrates

Microscope slides (3 × 1 in. SF10 glass, Schott Glass Technology) were immersed in piranha solution (sulfuric acid : hydrogen peroxide = 70 : 30 vol%) for 2 min prior to metal evaporation. The slides were rinsed with water several times and dried with nitrogen. Gold films were then deposited on the clean SF10 slides in an Edwards (Auto306) evaporator using chromium binder layers, which improved the adhesion between gold and SF10 glass. Then, they were stored under vacuum until used. It is well known that the high polarizability of the gold surface maximizes the attractive potential, which enables vesicles to remain intact and stable on the gold surface.[5] Therefore, each gold substrate was treated with oxygen plasma at 80 W for 5 min (March Plasmod Plasma Etcher, March Instruments) prior to vesicle immobilization.

Surface plasmon resonance (SPR) measurements

The plasma-treated gold substrate was attached to a SF10 right-angle prism (1.5 × 1.5 cm, Esco Products Inc.) using index matching fluid (n = 1.730 ± 0.0005, R. P. Cargille Laboratories, Inc.). A Teflon cell that holds the Tris buffer was placed in contact with the gold substrate. Both the prism and the cell were mounted on a rotating plate (two-circle goniometer 415, Huber Diffraktionstechnik GmbH & Co.) and rotated from 50 to 80° while a diode laser (LDCU5/4953, λ = 658 nm, 30 mW, Power Technologies) illuminated p-polarized light through the prism onto the gold substrate and Tris buffer through the O-ring in the middle of the cell. Data were recorded and analyzed using a home-written program and the light reflected from the gold substrate was viewed by a photodiode detector (201/579-7227, Thorlabs Inc.) and a CCD camera (C2400-08, Hamamatsu).

Results and discussion

Vesicles attacked by amphipathic helix peptides (AHP)

Fig. 1A and 1B show angle-resolved and time-resolved SPR data obtained as lipid vesicles on the gold surface transform into lipid bilayers by attack of the amphipathic helix peptide (AHP). Data were collected using a home-built SPR instrument whose schematic is depicted in Fig. 1C.

Prior to injection of vesicles into the cell, the reflectivity was scanned as a function of angle (see Tris buffer on gold surface, Fig. 1A,a). The critical angle was found to be approximately 55°, as expected, and the SPR angle for this condition turned out to be 65.6°. The derivative, $\mathrm{d}/\mathrm{d}\theta$ (R/R_o), was calculated based on this curve to choose the angle where the detector would be located for the acquisition of time-resolved SPR data. The maximum sensitivity for recording the time-resolved data could be achieved at 64.2° (highest point of the inset in Fig. 1A). After the detector was moved to 64.2°, the reflectivity was measured in real time as we changed conditions on the gold surface (Fig. 1B,1). At 350 s, 30-nm POPC vesicles were injected into the cell (Fig. 1B,2). Then, R/R_o drastically increased from $\sim$0.18 to $\sim$0.42 in 30 min, owing to the adsorption of vesicles on the gold surface (Fig. 1B,2–3). Angle-resolved SPR data were obtained after the saturation of vesicles on gold (Fig. 1A,b) and after washing the surface with Tris buffer to remove any weakly bound vesicles from the detection area (Fig. 1A,c). A slight decrease in reflectivity was observed when the buffer solution was injected into the cell (Fig. 1B,3). However, the SPR signal recovered in 2 min, and angle-resolved SPR data before and after washing were identical. These facts implied that the slight drop was not because of surface change but because of turbulence generated by the buffer injection into the cell and that the vesicles remained on the plasma-treated gold surface, forming a monolayer caused by a strong hydrophilic attraction between the vesicles and the pseudo-oxidized gold. This interaction shifted the SPR angle by 1.4° (from 65.6° in Fig. 1A,a to 67° in Fig. 1A,b,c).

After the formation of POPC vesicle layer on gold, we dispersed AHP on top of the layer (Fig. 1B,4). Initially, reflectivity increased to $\sim$0.45, and then gradually dropped to $\sim$0.28 and stabilized around that value (Fig. 1B,4–5). After stabilization, angle-scanned SPR data were obtained to check the SPR angle change (Fig. 1A,d). The angle was shifted to a lower value, 66.2°. This shift proved that the dielectric constants of the surface components were changed, which could correspond to a change in surface thickness. Whatever the exact behavior, the data implied that the added AHP had reacted with vesicles on the surface to transform the properties of materials on the surface. This will be discussed in more detail in the following section.

Next, the surface was washed with Tris buffer again to remove any residual species. The SPR curve measured after wiping away the unbound molecules on the surface with Tris

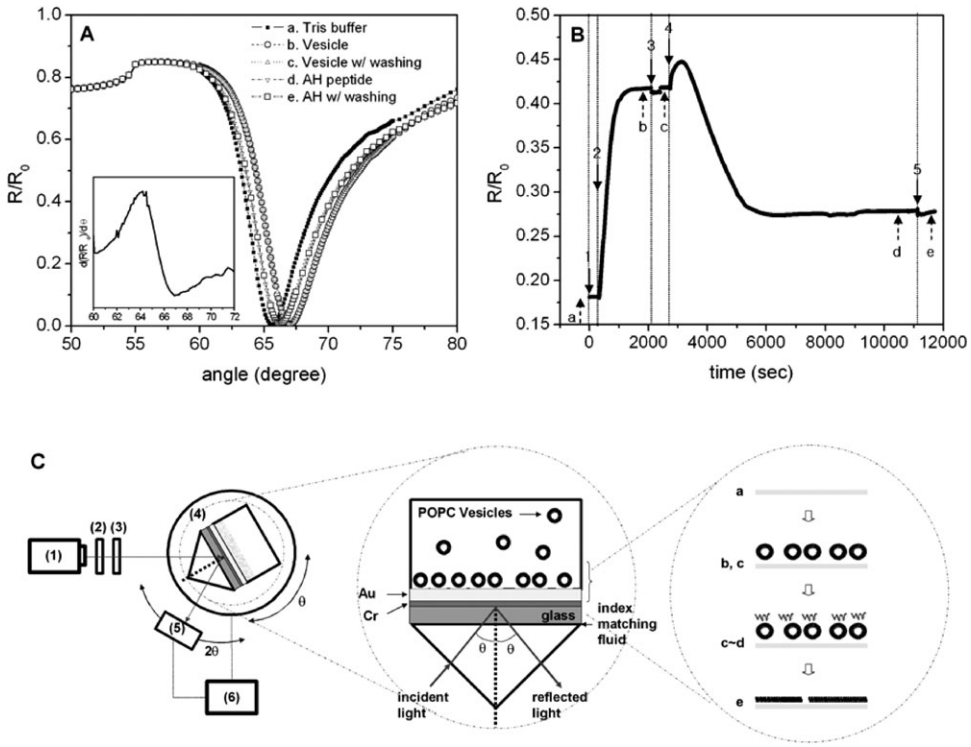

Fig. 1 (A) Angle-resolved SPR data obtained for each condition: (a) gold surface in buffer, (b) gold surface saturated with POPC vesicles, (c) condition b after washing with Tris buffer, (d) gold surface saturated with POPC bilayer after vesicle rupture by the injection of AHP, and (e) condition d after washing with Tris buffer. (B) Time-resolved SPR data obtained as vesicles rupture to form bilayers on plasma-treated gold surface: (1) injection of Tris buffer into a cell; (2) injection of POPC vesicles; (3) washing with Tris buffer; (4) injection of AHP; (5) washing with Tris buffer. (C) Schematic diagram of a SPR setup. Incoming light is reflected to a detector by the gold film, which is evaporated on SF10 glass. When the rotation stage turns by an angle θ, the detector moves by 2θ, (1) laser; (2) polarizer; (3) convex lens; (4) rotation stage; (5) detector; (6) computer; and (7) Teflon flowcell.

buffer proved again that the surface condition was not changed by washing (Fig. 1A,e).

Vesicle-rupture mechanism caused by amphipathic helix peptide (AHP)

The reflectivity changes in time-resolved SPR curves up to 4 are quite clear. Reflectivity (R/R_o) on bare gold stayed stable around 0.18 until vesicles were injected. Right after the injection, R/R_o dramatically increased owing to the adsorption of vesicles on gold. Once the surface was saturated, reflectivity became stable again, even after washing. However, after the injection of AHP, it behaved a little differently. For the first 10 min, it was increased by the adsorption of AHP onto the vesicle layers. We find this time delay quite remarkable. Then R/R_o gradually decreased instead of becoming stabilized at the increased level. It appears that interactions other than adsorption are taking place during this period. We propose a vesicle-rupture mechanism, as shown in Fig. 2 in terms of the perturbation free energy theory introduced by Zemel *et al.*[6] Fig. 2A represents the surface status before AHP injection (equivalent condition to Fig. 1A,c). Once the peptides are injected, they initially bind to the membrane surface of the vesicle, embedding their hydrophobic faces into the hydrocarbon core of the membrane (Fig. 2B). As more peptides approach the membrane, they form self-associated dimers or multimers in an energetically optimal state (Fig. 2C). Pore formation results from subsequent peptide crowding, oligomerization, and eventual reorientation along the membrane normal, which provides the lowest perturbation energy state (Fig. 2D). *In vivo*, viruses are ready to release their genetic cargos inside the cell at this stage through the tunnel generated at the cell membrane (Fig. 2b). In our case, ~10 min elapsed between the injection of AHP and the formation of pores (Fig. 1B). Interestingly, this time period matches well with the "several minutes" of the intermediate state that Melikyan *et al.*[1] reported for virus attack, which implies that peptides adsorbed at the surface actually take time to rearrange themselves so that they are ready to attack the membrane. In our opinion, this intermediate state is an important characteristic of each AHP or virus, and its duration deserves to be studied more deeply for the possible development of antiviral drugs.

What follows is a speculation about how the intact vesicle is transformed into a bilayer. With addition of more peptides, more pores are formed randomly on the membrane. The peptide may function as an edge-actant that can minimize line tension in a pore and allow the pores formed to move on the vesicle surface (Fig. 2E). As they draw close, the pores grow and coalesce, which may increase the mechanical stress on the vesicle's surface. When the stress becomes large enough, the vesicle bends toward the gold surface and rearranges to form a bilayer (Fig. 2F–G). This process takes much longer to occur

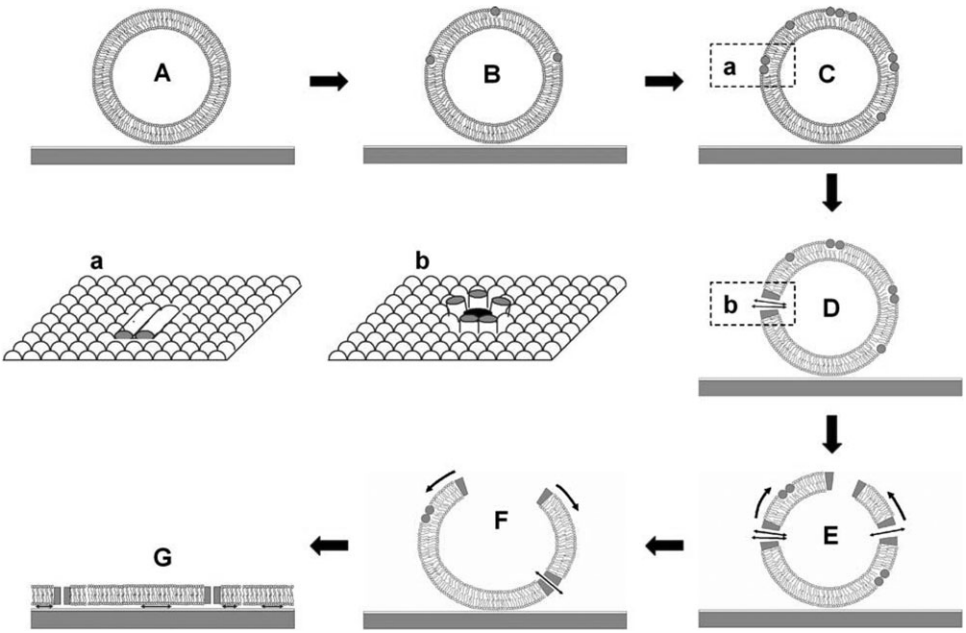

Fig. 2 Schematic of the vesicle-rupture mechanism for attack of AHP on a POPC vesicle. (A) Vesicle on the gold surface, (B–C) AHP-embedded vesicle, (D) vesicle with pores formed by reorientation of embedded AHPs, (E–F) vesicle attacked by AHPs, and (G) bilayer formed on gold surface. Peptides embedded (a) parallel and (b) normal to the surface of the vesicle.

(about 50 minutes). Based on this mechanism, we can guess that the lipid states at the highest peak, at the gradually decreasing slope, and at the stabilized state in Fig. 1B would be like what is pictured in Fig. 2D, E–F and G, respectively. The exact behavior for vesicle rupture by the amphipathic helix peptide is presently unknown and is the topic of future study.

Dielectric constants and thicknesses of lipid bilayers and lipid vesicles

In order to understand the status of lipids on a gold surface in more detail, the thickness (d) and the dielectric constants (ε') of POPC layers at each condition were estimated by fitting data in Fig. 1A using multi-phase theory.[7,8] Prior to the estimation of properties for lipid layers, we calculated the dielectric constants (ε'_{Au} and ε''_{Au}) and thickness (d_{Au}) of the gold film used for this experiment. (We use the convention that the real part of the dielectric constant is denoted by a superscript prime and the imaginary part by a superscript double prime.) The parameters were easily estimated by an iteration method using the known dielectric constant of SF10 prism, ε'_{pr}, calculated from the refractive index provided by the manufacturer, and the dielectric constant of Tris buffer, ε'_{buffer}. The best fit to Fig. 1A,a provided −11.8993 and 1.3715 for ε'_{Au} and ε''_{Au} and 49.2 nm for d_{Au}. This thickness was reasonable compared to the evaporation target (~50 nm), and these numbers were fixed for the following estimations of the optical properties and thicknesses of lipid layers.

With ε'_{pr}, ε'_{Au}, ε''_{Au}, ε'_{buffer} and d_{Au} fixed, the combinations of ε'_{lipid} and d_{lipid} that satisfy the fit to Fig. 1A,e were obtained as shown in Fig. 3A. Assuming that finally formed lipid on the gold surface is no more than a bilayer[4], 2.0262 could be easily deduced as a final value for ε'_{lipid} of the lipid bilayer of 5.3 nm.[9] The estimation of dielectric constants of vesicles is somewhat challenging because no one to our knowledge has ever estimated them, and their values are quite dependent upon the vesicle size and its surface coverage. Through the same approach we used to estimate dielectric constants of the

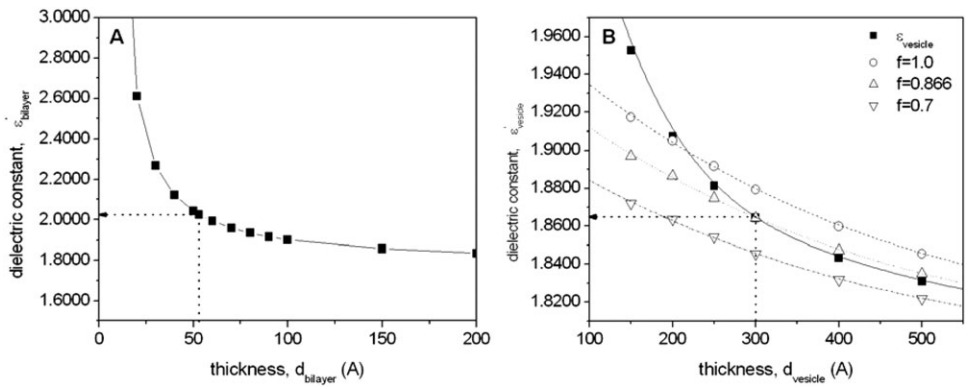

Fig. 3 Plot of dielectric constant *versus* thickness for (A) lipid bilayer and (B) vesicle layer.

Table 1 Dielectric functions (ε', ε'') and layer thicknesses (d) of multilayered samples including lipid membranes. The numbers represent best fits and are only rough estimates

Samples	ε'_{pr}	ε'_{Au}	ε''_{Au}	ε'_{lipid}	ε''_{lipid}	ε'_{buffer}	d_{Au}/nm	d_{lipid}/nm
Au–buffer				—	—			—
Au–vesicle–buffer	2.9687	−11.8993	1.3715	1.8593[a]	0	1.7664	49.2	31.9[a]
				1.8642[b]	0			30.0[b]
Au–bilayer–buffer				2.0262	0			5.3

[a] For a surface coverage of 0.85. [b] For a surface coverage of 0.866.

POPC bilayer, we obtained the plot between $\varepsilon'_{vesicle}$ and $d_{vesicle}$, as shown in Fig. 3B (■). Assuming that the vesicles are all unilamellar and spherical with a 30 nm diameter [$2r$ in eqn (1)], and form a monolayer on the gold surface, we calculated the dielectric constant of vesicles on the surface as follows:

$$f_{lipid} = \frac{4\pi(r^3 - (r - d_{lipid})^3)}{3(2r)^3} \quad (1)$$

$$\varepsilon'_{vesicle} = f_{lipid}\varepsilon'_{lipid} + (1 - f_{lipid})\varepsilon'_{buffer} \quad (2)$$

$$\varepsilon'_{measured} = f\varepsilon'_{vesicle} + (1 - f)\varepsilon'_{buffer} \quad (3)$$

where f_{lipid} and d_{lipid} are the fraction of lipid in a vesicle and the lipid thickness, respectively.

Two lines in Fig. 3B represent the plots of $\varepsilon'_{vesicle}$ *vs.* $d_{vesicle}$ when the surface coverage, f, is 1.0 (○) and 0.70 (▽), respectively. The plots for 70% < coverage < 100% can be proportionally distributed between Fig. 3B (○) and Fig. 3B (▽). Then, the dielectric constant of the lipid vesicles, $\varepsilon'_{vesicle}$, can be estimated from the curve (■) calculated from Fig. 1A,e, the surface coverage, and the vesicle size. With vesicle size fixed at 30 nm, the vertical line from 30 nm meets with Fig. 3B (■) when the surface coverage is 86.6%. This cross point leads to 1.8642 for the value of the dielectric constant of vesicles on gold. With the surface coverage fixed at 85%, we estimate dielectric constant and thickness to be 1.8593 and 31.9 nm, respectively. These data are summarized in Table 1. The numbers represent the best fit, and the numbers of digits given are for the assumptions stated above. These values, although given to many figures, are only meant as rough estimates. These estimates are consistent with what is expected for lipid bilayer formation.

Two-dimensional lipid pattern induced by virus-mimetic strategy

In the previous section we explained how a lipid vesicle is attacked by an AHP. Based on the same concept, we demonstrate that a lipid pattern can be built on a gold surface. A cross-patterned PDMS stamp was prepared as follows. GE Silicones components RTV615A (linear polymer) and RTV615B (containing cross-linking agent) were combined in a 10 : 1 (wt%) ratio and mixed thoroughly for 2 min. The mixture was degassed in a vacuum desiccator for 1 h. It was then spin-coated onto the wafer with cross patterns of 50-μm lines with 300-μm pitch. We cured the polymer film at 80 °C for 3 h in an oven. Then, the pattern area was cut to be used as a stamp. The patterned area of the PDMS stamp was immersed in a solution of AHP for ~1 min and placed on a plasma-treated gold surface (Fig. 4A,a) with finger pressure as shown in Fig. 4B,b. A line pattern of AHP was generated on the gold surface. After mounting the gold slide on our SPR setup and moving the detector to 64.2°, where the derivative of the reflectivity was the maximum, the buffer in the cell was replaced with the 30-nm POPC vesicle solution. Then, SPR microscopy was used to monitor the surface for 90 min. As the surface condition changed (Fig. 4B,b and C,c), the brightness of the whole imaging area increased with lipid attachment. Then, it reverted slightly to the dark side as vesicles in contact with AHP ruptured to form bilayers (Fig. 4D,d). This change in brightness corresponded to the reflectivity changes shown in Fig. 1B, although the brightness change was less dramatic.

To identify the difference more distinctly, the intensity of the image captured at 0 s (condition of Fig. 4B,b) was subtracted from that of the image captured at 90 min (condition of Fig. 4D,d) to create Fig. 5. In Fig. 5 we can clearly distinguish between square areas where vesicles remain, keeping a spherical surface, and lines where vesicles rupture to decrease the reflectivity. These two effects result in the formation of a two-dimensional lipid pattern with vesicle islands and bilayer lines.

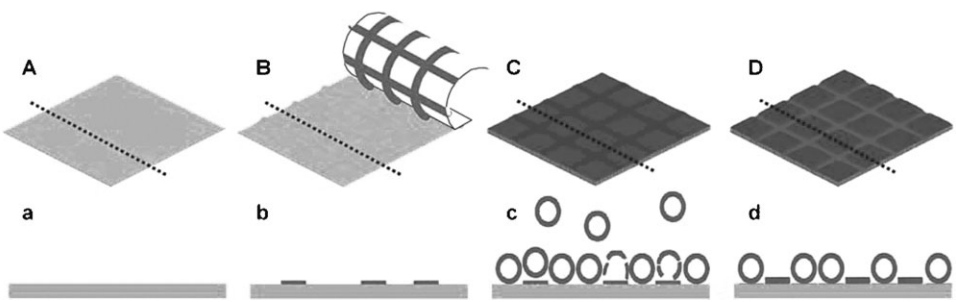

Fig. 4 Procedure for creating a two-dimensional lipid pattern. (A) Gold surface, (B) micro-stamping of AHP pattern, (C) adsorption of POPC vesicle onto AHP-patterned surface, and (D) completed two-dimensional lipid pattern.

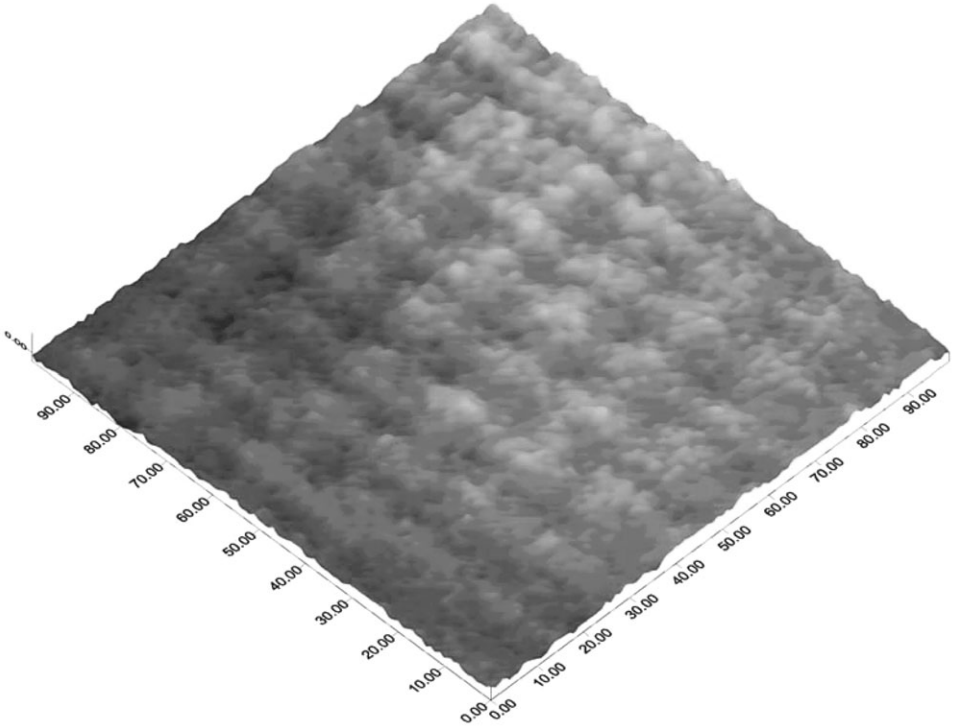

Fig. 5 SPR image of a two-dimensional lipid pattern showing vesicle islands and bilayer lines.

However, the reflectivity change between those two was smaller than expected. One reason for this might be the lateral mobility of the vesicles on gold induced by a slight gap ($\sim$1 nm) between the gold surface and the vesicles. In biological membranes, lateral mobility of membrane-associated molecules is actually important for their functions; therefore, lateral mobility has often been regarded as a criterion for the successful reconstitution of artificial membranes on solid supports. But in this experiment, this mobility may have caused an ambiguous interface between vesicles and bilayers. A second possibility that could account for the lack of contrast is the shortage of AHP patterned on the gold surface. In Fig. 1B, we provided more AHP than required to rupture vesicles on the surface, but here AHP was limited to the line pattern. Therefore, vesicles in Fig. 5 partially ruptured at the bottom interface where vesicles are in contact with AHP, which would have resulted in smaller changes in reflectivity than we estimated from Fig. 1B. Nevertheless, to the best of our knowledge, this is the first two-dimensional pattern generated with the combination of vesicles and bilayers, and it may prove useful in studying lipid mobilities. We have demonstrated that the pattern can be monitored *in situ* using SPR techniques without fluorescent tags. We anticipate that this capability will make many lipid systems accessible for new studies.

Conclusions

With vesicles made from 1-palmitoyl-2-oleoyl-*sn*-glycero-3-phosphocholine and PEP1 amphipathic helix peptide as a mimic for viral infection, we could investigate and predict the interaction between viruses and cell membranes using surface plasmon resonance (SPR) microscopy. The results of this study enabled us to propose a vesicle-rupture mechanism of amphipathic helix peptide, to provide optical properties of lipids of different formats (vesicles and bilayers) and to create a two-dimensional lipid pattern with vesicle islands and bilayer lines.

Acknowledgements

We greatly thank N. J. Cho for providing POPC vesicles and AHP. This work was supported by the National Science Foundation under grant number PHYS-0411641.

References

1 G. B. Melikyan, R. J. O. Barnard, L. G. Abrahamyan, W. Mothes and J. A. T. Young, *Proc. Natl. Acad. Sci. U. S. A.*, 2005, **102**, 8728.
2 R. M. Markosyan, F. S. Cohen and G. B. Melikyan, *Mol. Biol. Cell*, 2005, **16**, 5502.
3 M. Elazar, K. H. Cheong, P. Liu, H. B. Greenberg, C. M. Rice and J. S. Glenn, *J. Virol.*, 2003, **77**, 6055.
4 N. J. Cho, S. J. Cho, K. H. Cheong, J. S. Glenn and C. W. Frank, *J. Am. Chem. Soc.*, 2007, **129**, 10050.
5 C. A. Keller and B. Kasemo, *Biophys. J.*, 1998, **75**, 1397; C. A. Keller, K. Glasmastar, V. P. Zhdanov and B. Kasemo, *Phys. Rev. Lett.*, 2000, **84**, 5443; E. Reimhult, F. Hook and B. Kasemo, *Langmuir*, 2003, **19**, 1681.
6 A. Zemel, A. Ben-Shaul and S. May, *Eur. Biophys. J.*, 2005, **34**, 230.
7 S. Chah, E. Hutter, D. Roy, J. H. Fendler and J. Yi, *Chem. Phys.*, 2001, **272**, 127.
8 E. Hutter, J. H. Fendler and D. Roy, *J. Appl. Phys.*, 2001, **90**, 1977.
9 K. C. Duong-Ly, V. Nanda, W. F. DeGrado and K. P. Howard, *Protein Sci.*, 2005, **14**, 856.

